Unexpected Products of the Reaction of Cyanoacetylhydrazones of Aryl/heteryl Ketones with Hydrazine: A New Route to Aryl/Heteryl Hydrazones, X-ray Structure, and *In vitro* Anti-proliferative Activity against NCI 60-cell Line Panel

Reham A. Mohamed-Ezzat[1*], Benson M. Kariuki[2], Galal H. Elgemeie[3]

[1]Chemistry of Natural & Microbial Products Department, Pharmaceutical and Drug Industries Research Institute, National Research Centre, Cairo, 12622, Egypt [2]School of Chemistry, Cardiff University, Main Building, Park Place, Cardiff CF10 3AT, UK [3]Department of Chemistry, Faculty of Science, Helwan University, Cairo, 11795, Egypt

Abstract

A new unexpected synthetic non-catalytic method for the synthesis of novel heteryl hydrazones for base-modification of nucleoside analogs has been developed. Characterizations of the products have been performed using NMR spectroscopy and single crystal x-ray diffraction analysis. Further *in vitro* anti-proliferative potency of the compounds against NCI 60 cell lines has been estimated. The results indicate anti-cancer activity by the compounds against several of the cancer cell lines.

Keywords: Crystal x-ray; hydrazons; heteryl hydrazons; *in vitro* anti-proliferative activity.

1 Introduction

Hydrazone compounds are versatile materials with important applications including as intermediates in the development novel compounds. The compounds have wide-ranging impact in chemistry and bioscience [1-12]. With appropriate design, synthesis and understanding of their structure-activity relationship, a range of compounds with a diversity of desirable bio-activities can be developed. The materials possess a range of pharmacological and biological properties including antimicrobial, anti-tubercular, analgesic, anti-inflammatory, antiviral, antiplatelet, anticancer, antimalarial, cardioprotective, antihelmintic, anticonvulsant, antiprotozoal [13], antitrypanosomal [14], and anti-schistosomiasis activity [15].

Hydrazone compounds are associated to ketones and aldehydes through replacing the carbonyl oxygen with the hydrazinylidene group to produce a category of structures with the formula, $R_1(R_2)C=NNH_2$ [16,

*Corresponding author e-mail: reham_amgad_2010@yahoo.com.; ra.mohamed-ezzat@nrc.sci.eg; (Reham A. Mohamed).

17]. The compounds possess the (C=N) bond which is conjugated with the lone pair of electrons of the functional nitrogen atom [18]. Combination of the hydrazones with the other functional groups results in the generation of compounds with unique chemical & physical features [19]. In addition, the pharmacological properties may be enhanced by complexation with a metal [20].

Figure 1 shows some examples of anticancer agents comprising hydrazones. Potency against the Hl-60 human promyelocytic leukemic cell line has been reported for acylhydrazones such as compound **1** [21]. Compound **2** is reported to possess in vitro anti-cancer potency against the MCF-7 human breast cancer cell line [22]. The aryl hydrazone derivative (**3**) is described to possess an IC_{50} of 6.7 nM against MCF-7 & MDA-MB 231 breast cancer cell lines [23]. Other hydrazone derivatives such as compound **4** have a tendency to act against the lung cancer cell line (A549) [24]. The anticancer potency of the thiazolohydrazides (**5**) against prostate cancer has been assessed [25], also acetylpyridine and benzoylpyridine derived hydrazones (**6**, **7**) have been reported as agents against brain tumor [26].

The utility of hydrazones offers an opportunity for improved treatment through site-specific drug release in areas such as tumor tissue. Many researchers are experimenting on ways of generating hydrazones more efficiently, including using heat and chemical catalysts [27]. The importance of these moieties is illustrated by their use in the synthesis of numerous compounds of medicinal interest [28-30]. We have lately reported diverse synthetic methods for the preparation of heterocycles using cyanohydrazones [31-33]. Several derivatives of these ring structures are considered significant as antimetabolites in most biochemical reactions [34-36]. Beside an extensive range of new applications of the functionalized DNA in the biochemistry, attachment of reactive functional groups to nucleic acids is desired for bio-conjugates or further transformations. The introduction of a hydrazide or hydrazone group has been accomplished and the modified DNA was utilized for click chemistry. The hydrazide or the hydrazine functional group is a very useful group as a result of its extraordinary and unambiguous reactivity with various reagents [37]. In the light of this information and in the continuing results of our former research into the synthesis of biologically active heterocyclic compounds [38-41], the present paper reports an efficient and novel way to synthesize a hydrazone derivative with potential to play an essential role as an intermediate in the generation of many compounds. Conceivable clinical applications of these compounds include as anti-inflammatory and anticancer agents, in the prevention of platelet aggregation, and as chelating agents.

2 Results & discussion

2.1 Synthesis

This approach of synthesizing compound **11a-f** varies from other previously synthetic procedures [42]. Upon reacting hydrazine hydrate with 2-cyano-*N*′-(aryl/heteroarylethylidene)acetohydrazide (**8a-f**), compound **11a-f** was formed instead of the pyrazole derivative **12a-f.** Significant hydrazinolysis of amide bonds occurs without any catalyst. The reaction proceeds under reflux to give hydrazone **11a-f** as a result of cleavage of the amide bond. To our knowledge, this is the first report of production of 2-(1-(aryl ethylidene)hydrazine by this method. The product that was crystallized and characterized via the X-ray diffraction measurement to confirm the structure. The ^1H NMR spectrum of **11c** showed CH_3 protons at δ 2.00 ppm and the free NH_2 protons appeared at δ 6.48 ppm.

2.2 Crystal structure

In the crystal, the molecule is essentially planar except for the amine and methyl hydrogen atoms (Figure 2). Neighbouring molecules interact through N-H…N hydrogen bonds with geometry (N2…N1=3.134(5)Å, and N2-H2N…N1=159(4)°) to form dimers. In the dimers, pairs of the hydrogen bonds related by inversion symmetry form rings with geometry $R_2^2(8)$ in graph set notation [43]. The dimers are linked to their neighbours by Br1…N2 contacts with a distance of 3.358(4) Å to form ribbons in the [101] direction.

2.3 *In vitro* Anti-proliferative activity

The *in vitro* anti-proliferative activity against NCI-60 cell line panel was estimated. The compounds were selected via the National Cancer Institute "NCI", NIH through the Developmental Therapeutic Program for the determination of the *in vitro* anti-proliferative activity. This screen uses human tumor cell lines, representing melanoma, lung, leukemia, ovary, colon, brain, kidney, prostate and breast cancers.

The service of the NCI screening prioritises structures having a mode of action behaves as drugs on the bases of the computer-aided design (CAD). The ability of the submitted structures to bring the assortment to the collection of the NCI small molecules is essential to select them for the program of screening.

The compounds were assigned NCI codes NSC D-839209, NSC D-839207, NSC D-832401, NSC D-839205 & NSC D-839208 signifying the chemo type of this study. It was estimated at initial 10 μM one dose percent inhibition assay. The results's expression is represented as growth percent for the estimated compound on each cell line. The results are shown in figures (3-6) & table 1 indicate the lowest cell growth promotion for selected compounds.

The lowest cell growth promotion for compound **11a** was against breast cancer T-47D (GP = 65.06%), renal cancer CAKI-1 (GP = 82.64%), CNS cancer SNB-75 (GP= 89.80%), melanoma UACC-62 (GP = 90.26%), and NCI-H522 of the non-small cell lung cancer (GP = 92.83 %). Also the lowest cell growth promotion for compound **11b** was against breast cancer T-47D (GP = 82.48%), Renal cancer CAKI-1 (GP = 83.73%), non-small cell lung cancer HOP-62 (GP = 85.60 %), ovarian cancer SK-OV-3 (GP = 86.08%), CNS cancer SNB-75 (GP= 88.65%), and melanoma UACC-62 (GP = 90.79%).

The lowest cell growth promotion for compound **11c** was against leukemia HL-60(TB) cell line (GP = 89.92 %), and non-small cell lung cancer EKVX (GP = 94.48 %), colon cancer HCT-15 (GP = 98.40 %), CNS cancer SNB-19 (GP = 93.98 %), renal cancer UO-31 (GP = 91.59%), and breast cancer MCF7 (GP = 92.75%). The screening results thus show that hydrazone exhibited anti-cancer activity at 10 μM concentration against several of the cancer cell lines tested.

The lowest cell growth promotion for compound **11d** was against ovarian cancer cell line (GP = 72.47%), renal cancer (GP = 82.79%)**,** breast cancer MDA-MB-231/ATCC (GP = 84.34%), CNS cancer SNB-19 (GP = 95.36%), non-small cell lung cancer HOP-62 (GP = 95.43%), & melanoma UACC-62 (GP = 98.53%).

Moreover, compound **11f** reveals the lowest cell growth promotion against breast cancer T-47D (GP = 70.32%), non-small cell lung cancer HOP-62 (GP = 82.54%), renal Cancer CAKI-1 (GP = 86.84%), ovarian cancer SK-OV-3 (GP = 89.75%), CNS cancer SNB-75 (GP = 91.07%), melanoma SK-MEL28 (GP = 94.95%).

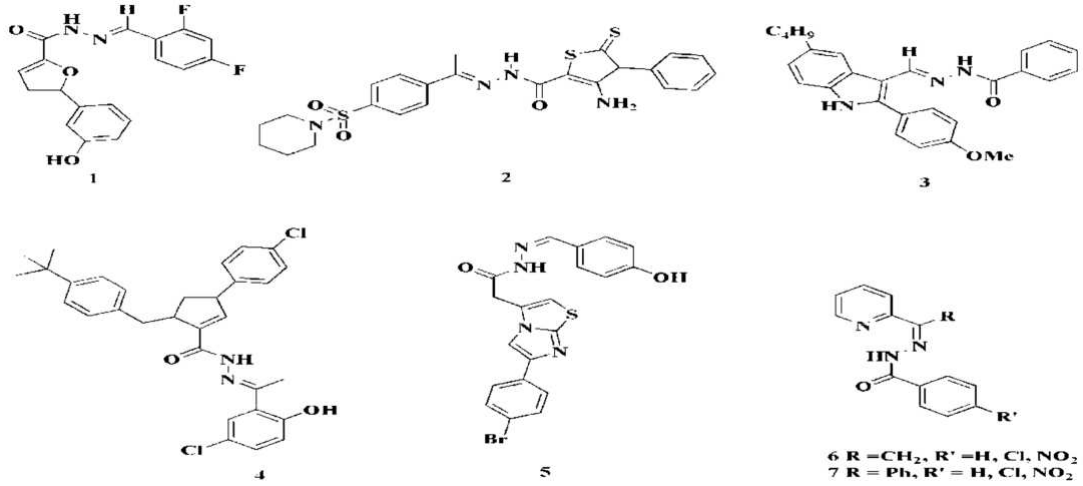

Figure.1: Structures of anticancer agents comprising hydrazones

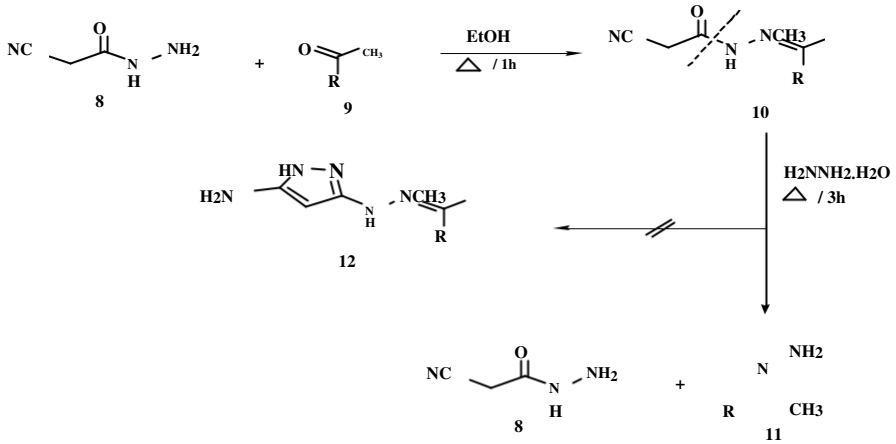

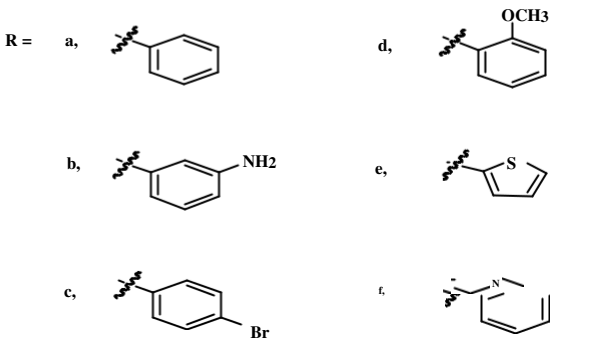

Scheme 1: Synthetic route for compound **11a-f**

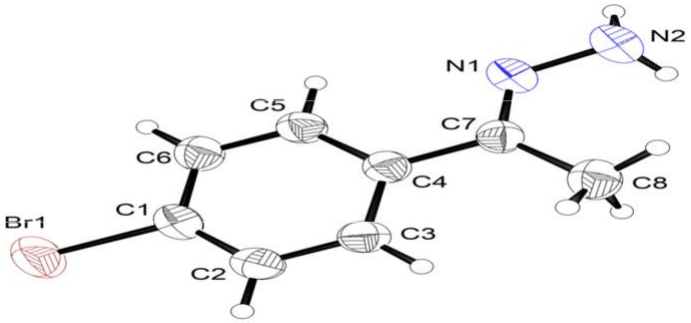

Figure 2: Molecule's ORTEP representation of compound **11c** in the crystal

Table 1

Crystal data & structure refinement for compound **11c**

Formula	$C_8H_9BrN_2$
Formula weight	213.08
Temperature	296(2) K
Wavelength	1.54184 Å
Crystal system	Monoclinic
Space group	$P2_1/c$
a	9.5991(6) Å
b	14.1926(9) Å
c	6.3214(4) Å
b	92.143(5)°
Volume	860.60(9) $Å^3$
Z	4
Density (calculated)	1.645 Mg/m^3
Absorption coefficient	5.982 mm^{-1}
F(000)	424
Crystal size	0.309 x 0.132 x 0.132 mm^3
Theta range for data collection	4.610 to 76.052°.
Index ranges	-11<=h<=12, -15<=k<=17, -7<=l<=7
Reflections collected	3734
Independent reflections	1769 [R(int) = 0.0394]
Completeness to theta = 67.684°	99.8 %
Refinement method	Full-matrix least-squares on F^2
Data / restraints / parameters	1769 / 0 / 109
Goodness-of-fit on F^2	1.120
Final R indices [I>2σ(I)]	R1 = 0.0530, wR2 = 0.1647
R indices (all data)	R1 = 0.0639, wR2 = 0.1823
Largest diff. peak and hole	1.067 and -0.664 e.$Å^{-3}$

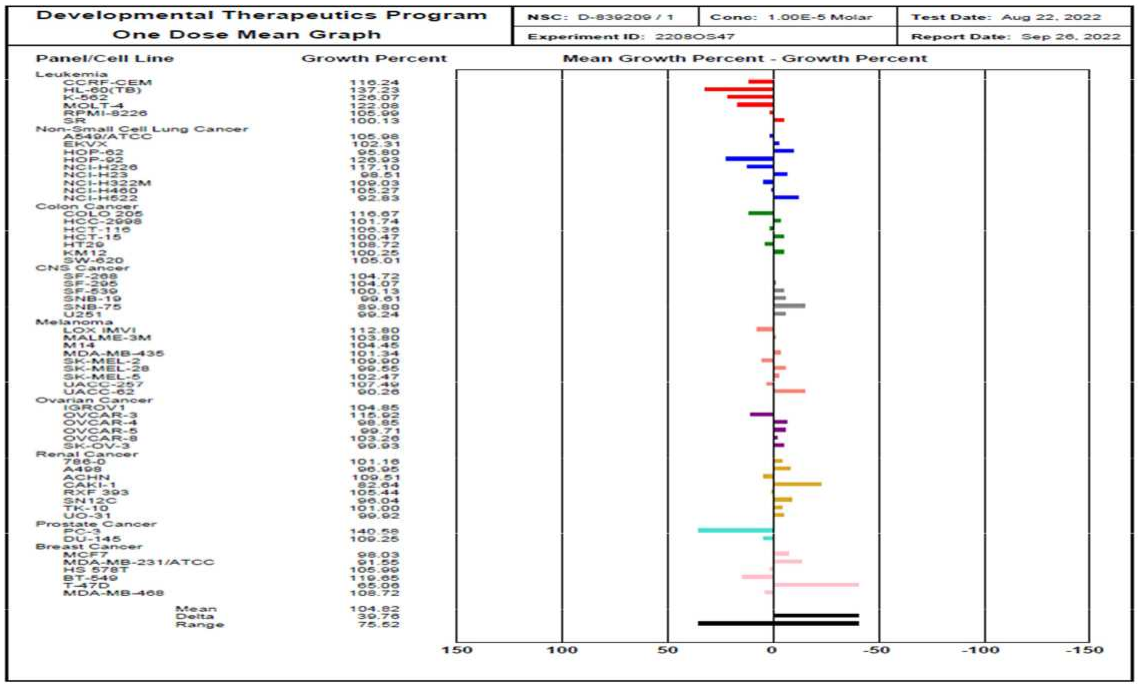

Figure 3: The data of the anti-cancer screening displayed for compound **11a**

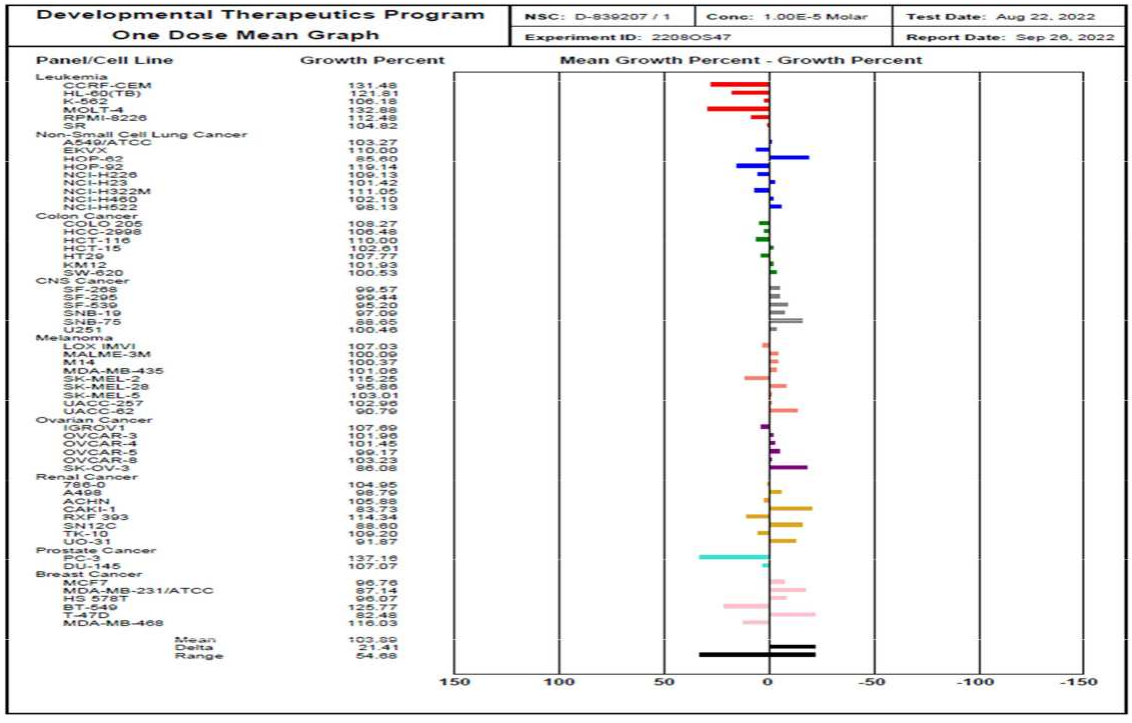

Figure 4: The data of the anti-cancer screening displayed for compound **11b**

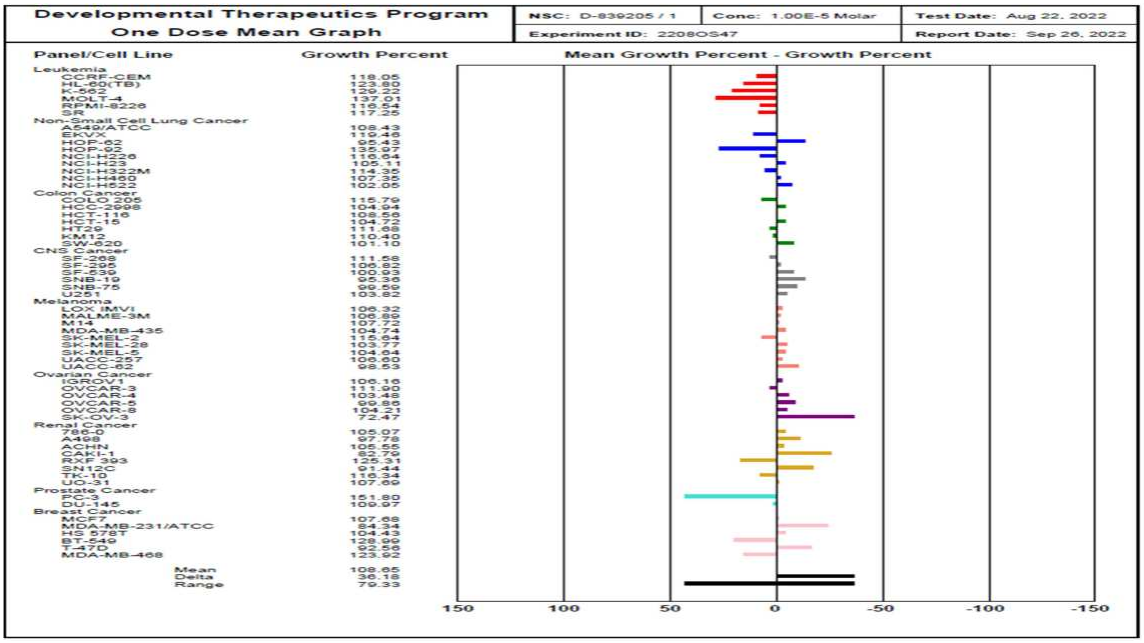

Figure 5: The data of the anti-cancer screening displayed for compound **11c**

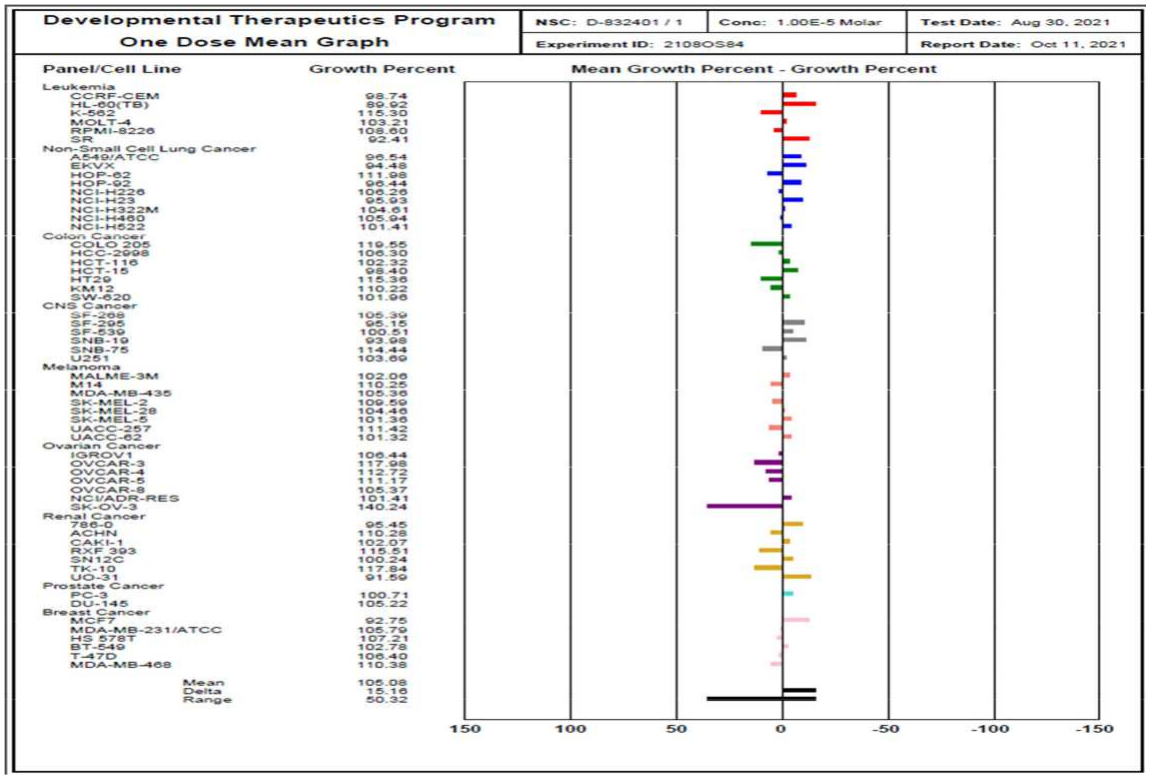

Figure 6: The data of the anti-cancer screening displayed for compound **11d**

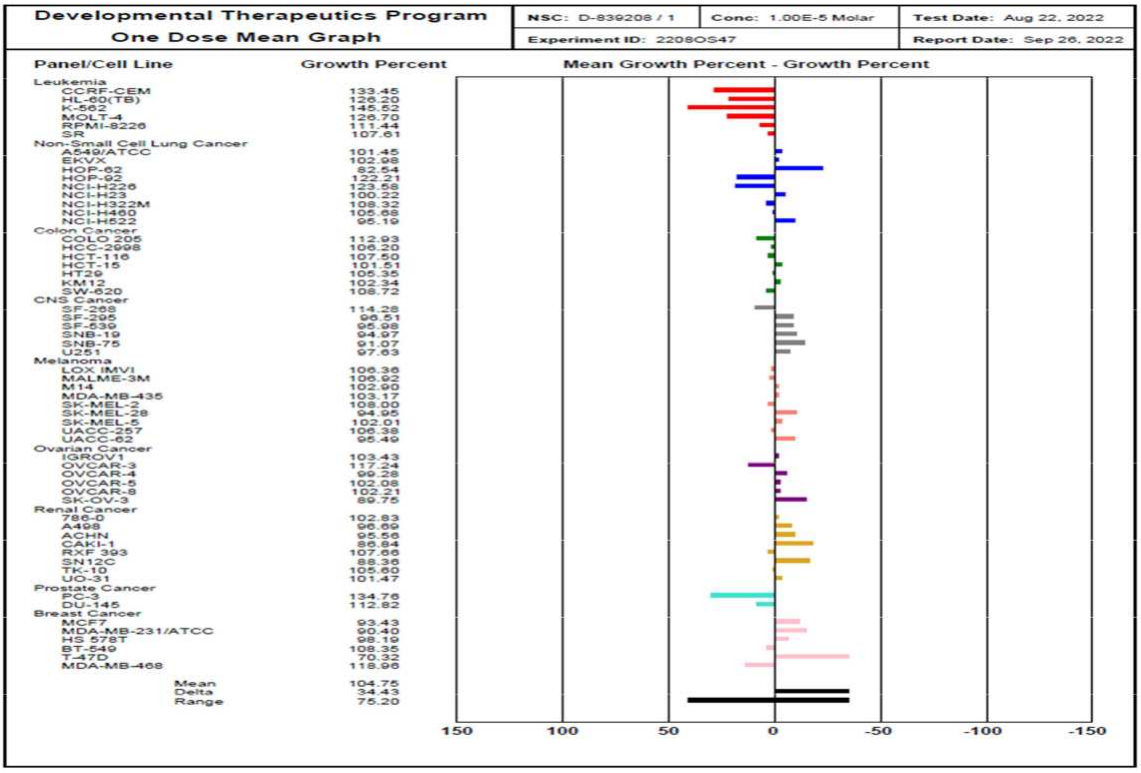

Figure 7: The data of the anti-cancer screening displayed for compound **11f**

Table 2

Antitumor determintions of the compounds using human tumor cell lines at a dose of 10 µM.

Panel/Cell line	**11a**	**11b**	**11c**	**11d**	**11f**
Leukemia					
CCRF-CEM	116.24	131.48	98.74	118.05	133.45
HL-60(TB)	137.23	121.81	89.92	123.80	126.20
K-562	126.07	106.18	115.30	129.22	145.52
MOLT-4	122.08	132.88	103.21	137.01	126.70
RPMI-8226	105.99	112.48	108.60	116.54	111.44
SR	100.13	104.82	92.41	117.25	107.61
Non-Small Cell Lung Cancer					

A549/ATCC	105.98	103.27	96.54	108.43	101.45
EKVX	102.31	110.00	94.48	119.46	102.98
HOP-62	95.80	85.60	111.98	95.43	82.54
HOP-92	126.93	119.14	96.44	135.97	122.21
NCI-H226	117.10	109.13	106.26	116.64	123.58
NCI-H23	98.51	101.42	95.93	105.11	100.22
NCI-H322M	109.03	111.05	104.61	114.35	108.32
NCI-H460	105.27	102.10	105.94	107.35	105.68
NCI-H522	92.83	98.13	101.41	102.05	95.19
Colon Cancer					
COLO 205	116.67	108.27	119.55	115.79	112.93
HCC-2998	101.74	106.48	106.30	104.94	106.20
HCT-116	106.36	110.00	102.32	108.56	107.50
HCT-15	100.47	102.61	98.40	104.72	101.51
HT29	108.72	107.77	115.36	111.58	105.35
KM12	100.25	101.93	110.22	110.40	102.34
SW-620	105.01	100.53	101.96	101.10	108.72
CNS Cancer					
SF-268	104.72	99.57	105.39	111.58	114.28
SF-295	104.07	99.44	95.15	106.82	96.51
SF-539	100.13	95.20	100.51	100.93	95.98
SNB-19	99.61	97.09	93.98	95.36	94.97
SNB-75	89.80	88.65	114.44	99.59	91.07
U251	99.24	100.46	103.69	103.82	97.63
Melanoma					
LOX IMVI	112.80	107.03	NT	106.32	106.36
MALME-3M	103.80	100.09	102.06	106.89	106.92
M14	104.45	100.37	110.25	107.72	102.90
MDA-MB-435	101.34	101.06	105.36	104.74	103.17
SK-MEL-2	109.90	115.25	109.59	115.64	108.00
SK-MEL-28	99.55	95.86	104.46	103.77	94.95

SK-MEL-5	102.47	103.01	101.36	104.64	102.01
UACC-257	107.49	102.96	111.42	106.60	106.38
UACC-62	90.26	90.79	101.32	98.53	95.49
Ovarian Cancer					
IGROV1	104.85	107.69	106.44	106.16	103.43
OVCAR-3	115.92	101.96	117.98	111.90	117.24
OVCAR-4	98.85	101.45	112.72	103.48	99.28
OVCAR-5	99.71	99.17	111.17	99.86	102.08
OVCAR-8	103.26	103.23	105.37	104.21	102.21
NCI/ADR-RES	NT	NT	101.41	NT	NT
SK-OV-3	99.93	86.08	140.24	72.47	89.75
Renal Cancer					
786-0	101.16	104.95	95.45	105.07	102.83
A498	96.95	98.79	NT	97.78	96.69
ACHN	109.51	105.88	110.28	105.55	95.56
CAKI-1	82.64	83.73	102.07	82.79	86.84
RXF 393	105.44	114.34	115.51	125.31	107.66
SN12C	96.04	88.60	100.24	91.44	88.36
TK-10	101.00	109.20	117.84	116.34	105.60
UO-31	99.92	91.87	91.59	107.69	101.47
Prostate Cancer					
PC-3	140.58	137.16	100.71	151.80	134.76
DU-145	109.25	107.07	105.22	109.97	112.82
Breast Cancer					
MCF7	98.03	96.76	92.75	107.68	93.43
MDA-MB-231/ATCC	91.55	87.14	105.79	84.34	90.40
HS 578T	105.99	96.76	107.21	104.43	98.19
BT-549	119.65	125.77	102.78	128.99	108.35
T-47D	65.06	82.48	106.40	92.56	70.32
MDA-MB-468	108.72	116.03	110.38	123.92	118.96

(*NT: Not tested)

3 Experimental

3.1 Chemical Methods. Monitoring of the reaction progress was performed with visualization under Ultra violet light using TLC through pre-coated silica gel 60 F_{245}aluminium plates. The melting points were measured using a Stuart SMP30 and were uncorrected. The measurements of the spectral data of the synthesized compounds were performed in Cairo University, Ain Shams University, & National Research Centre, Egypt. The ^{1}H NMR spectra were measured on a Bruker Fourier 400 & 500 (at 400 & 500 MHz, respectively) at 300 K.

3.2. Synthesis & crystallization

3.2.1. General procedure for synthesizing compounds 10a-e:

The substituted cyanoacetohydrazides **10** were furnished upon react the 2-cyanoacetohydrazide **8** (0.01 mol) with the acetophenone derivatives **9** (0.01 mol) for 5-10 minutes under reflux in ethyl alcohol (20 mL). The precipitate was filtered, and then re-crystallized using ethyl alcohol.

Compounds **10a** [44], **10e** [45] & **10f** [46, 47] were previously synthesized and reported in literature.

3.2.1.1. N'-(1-(4-bromophenyl)ethylidene)-2-cyanoacetohydrazide (10c)

Compound **10c** was afforded as a colorless crystals (93 %), 186-188°C; ^{1}H-NMR (400 MHz, DMSO-d_6): δ 2.26 (*s*, 3H, CH_3), 4.2 (s, 2H, CH_2), 7.61 (*d,* 2H, *J = 16 Hz*, 2CH), 7.75 (*d*, 2H, *J =8 Hz*, 2CH), 11.01 (*s*, 1H, NH). Analysis calculated for $C_{11}H_{10}BrN_3O$ (280.12): C, 47.16; H, 3.60; Br, 28.52; N, 15.00. Found: C, 47.15; H, 3.60; Br, 28.51; N, 15.00.

3.2.1.2. 2-cyano-N'-(1-(2-methoxyphenyl)ethylidene)acetohydrazide (10d)

Compound **10b** was afforded as colorless crystals (92 %), ^{1}H-NMR (500 MHz, DMSO-d_6): δ 2.13 (*s*, 3H, CH_3), 3.77-3.87 (m, 3H, OCH_3), 4.07 (s, 2H, CH_2), 6.92-7.03 (*m,* 3H, 3CH), 7.33-7.35 (*m*, 1H, 1CH), 10.90 (*s*, 1H, NH). ^{13}C-NMR (500 MHz, DMSO- d_6) δ (ppm): 18.39, 25.27, 56.07, 112.21, 116.65, 121.44, 129.83, 130.89, 131.44, 155.93, 156.04, 166.14. Analysis calculated for $C_{12}H_{13}N_3O_2$ (231.25): C, 62.33; H, 5.67; N, 18.17. Found: C, 62.31; H, 5.66; N, 18.15.

3.2.2. General procedure for synthesizing compounds 11a-e:

A mixture of the *N*'-(1-(aryl/heteroaryl)ethylidene)-2-cyanoacetohydrazide (**10**) (0.01 mol), hydrazine hydrate (0.01 mol) was allowed to reflux for 3 h in ethyl alcohol (10 mL). Some solvent was allowed evaporate and the solid product was filtered and then re-crystallized utilizing ethyl alcohol.

3.2.2.1. 1-(1-phenylethylidene)hydrazine (11a)

Compound **11a** was afforded as a yellow crystals (81 %), 120-121° C;IR (KBr, cm^{-1}): υ 3054 (ArCH), 1567 (C=C). ^{1}H-NMR (400 MHz, DMSO-d_6): δ 2.2 (*s*, 3H, CH_3), 3.3 (*s*, 2H, NH_2), 7.45–7.48 (*d,* 3H, CH), 7.95–7.99 (*d*, 2H, CH). ^{13}C-NMR (400 MHz, DMSO-d6) δ (ppm): 14.6, 126.4, 128.4, 129.7, 137.8, 157.2. Analysis calculated for $C_8H_{10}N_2$ (134.18): C, 71.61; H, 7.51; N, 20.88. Found: C, 71.59; H, 7.50; N, 20.87.

3.2.2.2. *2-(1-(3-aminophenyl)ethylidene)hydrazine (11b)*

Compound **11b** was afforded as a yellow crystals (78 %), 85-86° C;^{1}H-NMR (400 MHz, DMSO-d_6): δ 1.9 (*s*, 3H, CH_3), 4.9 (*s*, 2H, NH_2), 6.3 (*s*, 2H, NH_2), 6.4 (*d,* 1H, CH), 6.8 (*d*, 1H, CH), 6.96-6.99 (*m*, 2H, 2CH). ^{13}C-NMR (400 MHz, DMSO-d6) δ (ppm): 11.4, 110.5, 112.95, 112.98, 128.3, 140.4, 142.8, 148.2. Analysis calculated for $C_8H_{11}N_3$ (149.19): C, 64.40; H, 7.43; N, 28.16. Found: C, 64.40; H, 7.42; N, 28.15.

3.2.2.3. *2-(1-(4-bromophenyl)ethylidene)hydrazine (11c)*

Compound **11c** was afforded as a buff crystals (70 %), 77-78° C;[1] H-NMR (400 MHz, DMSO-d_6): δ 2.00 (*s*, 3H, CH_3), 6.48 (*s*, 2H, NH_2), 7.46–7.49 (*d,* 2H, 2CH), 7.57–7.55 (*d*, 2H, 2CH). ^{13}C-NMR (400 MHz, DMSO-d6) δ (ppm): 11.1, 120.0, 126.7, 128.5, 130.9, 131.4, 139.0, 140.7. Analysis calculated for $C_8H_9BrN_2$ (213.07): C, 45.09; H4.26; Br, 37.50; N, 13.15 %. Found: C, 45.09; H4.25; Br, 37.50; N, 13.14 %.

3.2.2.4. *1-(1-(2-methoxyphenyl)ethylidene)hydrazine (11d)*

Compound **11d** was afforded as a pink solid (76 %), >300° C;[1] H NMR (400 MHz, DMSO-d_6): δ not dissolved properly in the solvent. IR (KBr, cm^{-1}): υ 3171 (ArCH), 2343, 2050, 1980, 1542 (C=C), 1154 (C-O). Analysis calculated for $C_9H_{12}N_2O$ (164.2): C, 65.83; H, 7.37; N, 17.06. Found: C, 65.81; H, 7.36; N, 17.05.

3.2.2.5. 1-(1-(thiophen-2-yl)ethylidene)hydrazine (11e)

Compound **11e** was afforded as a yellow crystals (70 %), ^{1}H-NMR (400 MHz, DMSO-d_6): δ 2.03 (*s*, 3H, CH_3), 6.17 (*s*, 2H, NH_2), 6.96-6.98 (t, 1H, CH), 7.09-7.11 (d, 1H, CH), 7.29-7.30 (d,1H, CH). Analysis calculated for $C_6H_8N_2S$ (140.21): C, 51.40; H, 5.75; N, 19.98; S, 22.87%. Found: C, 51.40; H, 5.74; N, 19.97; S, 22.86%.

3.2.2.5. 1-(1-(pyridin-2-yl)ethylidene)hydrazine (11f)

Compound **11f** was afforded as a yellow crystals (54 %), >300°C;IR (KBr, cm^{-1}): υ 3240, 3125 (NH_2), 3023 (ArCH), 1533 (C=C). ^{1}H-NMR (400 MHz, DMSO-d_6): δ 2.2 (*s*, 3H, CH_3), 5.9 (*s*, 2H, NH_2), 7.2 (*t,* 1H, CH), 7.68- 7.69 (*t*, 1H, CH), 8.46-8.47 (d, 1H, 1CH), 9.34 (*d*, 1H, 1CH). ^{13}C-NMR (400 MHz, DMSO-d6) δ (ppm): 10.1, 151.0, 151.2, 151.5, 167.1. Analysis calculated for $C_7H_9N_3$ (135.17): C, 62.20; H, 6.71; N, 31.09. Found: C, 62.19; H, 6.70; N, 31.08.

3.3 Determination of the crystal structure

Collection of the Single crystal XRD data were performed on an Agilent SuperNova Dual Atlas diffractometer via a mirror mono-chromator utilizing Cu (λ = 1.5418 Å) radiation at ambient temperature. Utilizing SHELXS the crystal structure was solved [48] and then refined utilizing SHELXL [49]. Refinement of the non-hydrogen atoms carried out with the anisotropic displacement parameters. In idealized positions the hydrogen atoms were inserted, and a riding model was utilized with Uiso set at 1.2 or 1.5 times the value of Ueq for the atom to which they are bonded. The crystal and the refinement data are accomplished in table 2. The deposition of the crystal structure has been performed in the Cambridge Structural Database under reference CCDC 2087302.

3.4 *In vitro* Anti-proliferative activity

Primary anti-cancer assays were performed consistent with the NCI's protocol [50-54]. The compound was added at single concentration and then the incubation of the cell culture was carried out for forty eight hours. Sulforhodamine B (SRB), a protein binding dye, was utilized to identify the endpoints (SRB). The compound's results are expressed as the percent growth of the treated cells comparable to the un-treated cells of the control (Figure 3). Range of growth (%) indicated the highest & the lowest growth that found for several cancer cell lines in refer to the sensitivity against the cell lines at the primary single high dose (10^{-5}M).

4 Conclusions

2-(1-(Aryl/heteroaryl)ethylidene)hydrazines have been obtained by *non-catalytic* hydrazinolysis of amide. The reaction was performed using hydrazine monohydrate to cause amide bond-cleavage under reflux to yield the product. The compounds have been identified utilizing spectroscopic and single crystal X-ray diffraction measurements. Investigations of the *in vitro* anti-tumor activity of the products have been performed. The results indicate that the compounds exhibit anticancer activity against a variety of the cancer cell lines.

Acknowledgment: The authors thank the National Cancer Institute, Bethesda-Maryland, USA for performing the antitumor screening.

- The study was approved under number 13444052023 by the Medical Research Ethics Committee (MERC) fedral (accurance no. : FWA 00014747).

References

[1] Zhu, D.; Lv, L.; Li, C. C.; Ung, S.; Gao, J.; Li, C. J. Umpolung of carbonyl groups as alkyl organometallic reagent surrogates for palladium-catalyzed allylic alkylation. Angew Chem Int. Ed. Engl. 2018; 57: 16520-16524.

[2] Liu W, Twilton J, Wei B, Lee M, Hopkins MN, Bacsa J, Stahl SS, Davies HML. Copper-Catalyzed oxidation of hydrazones to diazo compounds using oxygen as the terminal oxidant. ACS Catal. 2021; 11(5): 2676–2683.

[3] Rahim F, Zaman K, Taha M, Ullah H, Ghufran M, Wadood A, Rehman W, Uddin N, Shah SAA, Sajid M, Nawaz F, Khan KM. Synthesis, in vitro alpha-glucosidase inhibitory potential of benzimidazole bearing bis-Schiff bases and their molecular docking study. Bioorg. Chem. 2020; 94: 103394.

[4] Chuit C, Corriu RJ, Reye C, Young JC. Reactivity of penta- and hexacoordinate silicon compounds and their role as reaction intermediates. Chem Rev. 1993; 93(4): 1371-1448.

[5] Elgemeie, GH, Alkhursani, SA, Mohamed, RA. New synthetic strategies for acyclic and cyclic pyrimidinethione nucleosides and their analogues. Nucleosides Nucleotides. 2019; 38: 12−87.

[6] Mohamed-Ezzat RA, Elgemeie GH, Jones PG. Crystal structures of (*E*)-2-amino-4-methyl-sulfanyl-6-oxo-1-(1-phenylethylideneamino)-1,6-dihydro pyrimidine-5-carbonitrile and (*E*)-2-amino-4-methylsulfanyl-6-oxo-1-[1-(pyridin-2-yl)ethylideneamino]-1,6-dihydropyrimidine-5-carbonitrile. Acta Cryst. 2021; E77: 547-550.

[7] Elgemeie, GH, Salah, AM, Abbas, NS, Hussein, HA, Mohamed, RA, Pyrimidine non-nucleoside analogs: A direct synthesis of a novel class of *N*-substituted amino and *N*-sulfonamide derivatives of pyrimidines, Nucleosides Nucleotides. 2017; 36: 213-223. https://doi.org/10.1080/15257770.2016.1257808.

[8] Mohamady S, Kralt B, Samwel SK, Taylor SD. Efficient One-Pot, Two-Component Modular Synthesis of 3,5-disubstituted pyrazoles. ACS Omega 2018: 3(11): 15566–15574.

[9] Coogan NT, Chimes MA, Raftery J, Mocilac P, Denecke MA. Regioselective synthesis of V-shaped Bistriazinyl-phenanthrolines. J. Org. Chem. 2015; 80(17): 8684-8693.

[10] Tripathi RK, Ayyannan SR. Design, Synthesis, and Evaluation of 2-Amino-6-nitrobenzothiazole-derived hydrazones as MAO inhibitors: Role of the Methylene Spacer Group. ChemMedChem. 2016; 11(14): 1551-1567.

[11] Souza LW, Squitieri RA, Dimirjian CA, Hodur BM, Nickerson LA, Penrod CN, Cordova J, Fettinger JC, Shaw JT. Enantioselective synthesis of indolines, benzodihydrothiophenes, and indanes by C−H insertion of Donor/Donor Carbenes. Angew. Chem. Int. Ed. 2018; 57(46): 15213-15216.

[12] Ma XD, Yang SQ, Gu SX, He QQ, Chen FE, De Clercq E, Balzarini J, Pannecouque C. Synthesis and anti-HIV activity of aryl-2-[(4-cyanophenyl)amino]-4-pyrimidinone hydrazones as potent non-nucleoside reverse transcriptase inhibitors. ChemMedChem. 2011; 6(12): 2225-2232.

[13] Rollas S, Küçükgüzel SG. Biological activities of hydrazone derivatives. Molecules. 2007; 12: 1910-1939.

[14] Narang R, Narasimhan B, Sharma S. A review on biological activities and chemical synthesis of hydrazide derivatives. Curr Med Chem. 2012; 19: 569-612.

[15] Negi VJ, Sharma AK, Negi JS, Ra V. Biological activities of hydrazone derivatives in the new millennium. Int J Pharm Chem. 2012; 4: 100-109.

[16] Uppal G, Bala S, Kamboj S, Saini M. Therapeutic review exploring antimicrobial potential of hydrazones as promising lead. Der Pharma Chem. 2011; 3: 250-268.

[17] Verma G, Marella A, Shaquiquzzaman M, Akhtar M, Ali MR, Alam MM. A review exploring biological activities of hydrazones. J Pharm Bioallied Sci. 2014; 6(2): 69-80.

[18] Corey EJ, Enders D. Applications of *N*, *N*-dimethylhydrazones to synthesis. Use in efficient, positionally and stereochemically selective C=C bond formation, oxidative hydrolysis of carbonyl compounds. Tetrahedron Lett. 1976; 17: 3-6.

[19] Xavier AJ, Thakur M, Marie JM. Synthesis and spectral characterisation of hydrazone based 14-membered octaaza macrocyclic Ni (II) complexes. J Chem Pharm Res. 2012; 4: 986-90.

[20] Banerjee S, Mondal S, Chakraborty W, Sen S, Gachhui R, Butcher RJ, et al. Syntheses, X-ray crystal structures, DNA binding, oxidative cleavage and antimicrobial studies of two Cu (II)

hydrazone complees. Polyhedron. 2009; 28: 2785-2793.
[21] Cui Z, Li Y, Ling Y, Huang J, Cui J, Wang R, et al. New class of potent antitumor acylhydrazone derivatives containing furan. Eur J Med Chem. 2010; 45: 5576-5584.
[22] Al-Said MS, Bashandy MS, Al-Qasoumi SI, Ghorab MM. Anti-breast cancer activity of some novel 1,2-dihydropyridine, thiophene and thiazole derivatives. Eur J Med Chem. 2011; 46: 137-141.
[23] Vogel S, Kaufmann D, Pojarová M, Müller C, Pfaller T, Kühne S, et al. Aroyl hydrazones of 2-phenylindole-3-carbaldehydes as novel antimitotic agents. Bioorg Med Chem. 2008; 16: 6436-6447.
[24] Zheng LW, Wu LL, Zhao BX, Dong WL, Miao JY. Synthesis of novel substituted pyrazole-5-carbohydrazide hydrazone derivatives and discovery of a potent apoptosis inducer in A549 lung cancer cells. Bioorg Med Chem. 2009; 17: 1957-1962.
[25] Gürsoy E, Güzeldemirci NU. Synthesis and primary cytotoxicity evaluation of new imidazo[2,1-*b*] thiazole derivatives. Eur J Med Chem. 2007; 42: 320-326.
[26] Despaigne AA, Parrilha GL, Izidoro JB, da Costa PR, dos Santos RG, Piro OE, et al. 2-Acetylpyridine-and 2-benzoylpyridine-derived hydrazones and their gallium (III) complexes are highly cytotoxic to glioma cells. Eur J Med Chem. 2012; 50: 163-172.
[27] Wahbeh J, Milkowski S. The Use of Hydrazones for Biomedical Applications. SLAS Technology 2019; 24(2): 161-168.
[28] Kim J, Khoo J, Lee J, Shin W, Choi S. Process for the preparation of pyrrolo[2,3-*c*]pyridine derivatives or pharmaceutically acceptable salts thereof. PCT Int. Appl. 2014; WO 2014189238 A1 20141127.
[29] Basawaraj R, Channamma M, Sangmeshwar W. Synthesis and antitubercular activity of 4-thiazolidinone derivatives incorporating benzofuran moiety. Indian J. Heterocycl. Chem. 2014; 24(1): 59-66.
[30] Chen F, Ma X, Gu S. Preparation of diaryl pyrimidinone hydrazone derivative for an antitumor and anti-HIV agents. Faming Zhuanli Shenqing 2011; CN 102153517 A 20110817.
[31] Elgemeie, GH, Mohamed, RA, Hussein, HA, Jones, PG. Crystal structure of *N*-(2-amino-5-cyano-4-methylsulfanyl-6-oxo-1,6-dihydropyrimidin-1-yl)-4-bromobenzene-sulfonamide dimethylformamide monosolvate, *Acta Crystallogr E Crystallogr Commun*. 2015; 71: 1322-1324. https://doi.org/10.1107/S2056989015018903.
[32] Elgemeie GH, Salah, AM, Mohamed, RA, Jones, PG. Crystal structure of (*E*)-2-amino-4-methylsulfanyl-6-oxo-1-{[(thiophen-2-yl)methyl-idene]amino}-1,6-dihydropyrimidine-5-carbo-nitrile, Acta Crystallogr E Crystallogr Commun. 2015; 71: 1319–1321.
[33] Azzam RA, Elgemeie, GH, Osman RR. Synthesis of novel pyrido[2,1-*b*]benzothiazole and *N*-substituted 2- pyridylbenzothiazole derivatives showing remarkable fluorescence and biological activities. J. Mol. Structure. 2020; 1201: 127194.
[34] Elgemeie, GH, Mohamed-Ezzat, RA. New Strategies Targeting Cancer Metabolism: Anticancer Drugs, Synthetic Analogues and Antitumor Agents. Edited by. Elgemeie, GH, Mohamed-Ezzat, RA. New Strategies Targeting Cancer Metabolism: Anticancer Drugs, Synthetic Analogues and Antitumor Agents, Elsevier, 2022, pp. 303-392, ISBN 9780128217832.
[35] Elgemeie, GH, Mohamed-Ezzat, RA, Chapter 10 - Synthetic strategies for antimetabolite analogs in our laboratory, Editor(s): Elgemeie, GH, Mohamed-Ezzat, RA, New Strategies Targeting Cancer Metabolism, Elsevier, 2022, pp. 547-611, ISBN 9780128217832.
[36] Mohamed-Ezzat RA, Kariuki, BM, Azzam RA. Morpholin-4-ium [5-cyano-6-(4-methylphenyl)-4-(morpholin-4-yl)pyrimidin-2-yl](phenylsulfon-yl)amide. IUCrData 2022; 7 (11): x221033.
[37] Raindlová V, Pohl R, Šanda M, Hocek M. Direct polymerase synthesis of reactive aldehyde-functionalized DNA and its conjugation and staining with hydrazines. Angew. Chem. 2010; 122: 1082-1084.
[38] Metwally NH, Elgemeie GH, Jones PG. Crystal structure of ethyl 2-(3-amino-5-oxo-2-tosyl-2,5-dihydro-1H-pyrazol-1-yl)acetate. Acta Cryst. 2021; E77: 615-617.
[39] Elgemeie, GH, Mohamed RA. Microwave chemistry: Synthesis of purine and pyrimidine nucleosides using microwave radiation. J. Carbohydr. Chem. 2019; 38: 1-47.
[40] Mohamed-Ezzat, RA, Kariuki, BM, Azzam, R A. Synthesis and crystal structure of *N*-(5-acetyl-4-methyl-pyrimidin-2-yl)benzene-sulfonamide. Acta Cryst. 2023; E79 (Pt 4): 331–334.
[41] Metwally NM, Elgemeie GH, Jones PG. Crystal structure of 2-{[5-amino-1-(phenylsulfonyl)-1H_pyrazol-3-yl]oxy}-1-(4-methylphenyl)ethan-1-one. Acta Cryst. 2021; E77: 1054-1057.
[42] Newkome GR, Fishel DL. Preparation of hydrazones: Acetophenone hydrazine. Org. Synth. 1970; 50: 102.
[43] Bernstein J, Davis RE, Shimoni L, Chang NL. Patterns in hydrogen bonding: functionality and graph set analysis in crystals. Angew. Chem., Int. Ed. 1995; 34: 1555-1573.
[44] Reinecke MG, Woodrow TA, Brown ES. Pyrazolo[3,4-*c*]pyridazines from hydrazine and aminothiophenecarboxylates. J. Org. Chem. 1992; 57 (3): 1018-1021.
[45] Al-Awadi NA, Elnagdi MH, Mathew T, Abdel Khalik M. Pyrolysis of aminonitriles, cyanohydrazones, and cyanoacetamides. Part II. Elimination reactions of arylacetylhydrazone, arylcyanoacetylhydrazone, and substituted cyanoacetamides. Int. J. Chem. Kinet. 1996; 28(10): 749-754.
[46] Khidre RE, El-Gogary SR, Mostafa MS. Design, synthesis, and antimicrobial evaluation of some novel pyridine, coumarin, and thiazole derivatives. J. Heterocycl. Chem. 2017; 54(4): 2511-2519.

[47] Abdel-Wahab, BF, Abdelbasset FA, Awad GEA, El-Hiti, GA. Lett Drug Des Discov. 2017; 14(11): 1316-1323.
[48] Sheldrick GM. A Short History of SHELX. Acta Crystallogr. A Found. Crystallogr. 2008; 64: 112–122.
[49] Sheldrick GM. Crystal Structure Refinement with SHELXL. Acta Crystallogr. C Struct. Chem. 2015; 71: 3–8.
[50] http://dtp.nci.nih.gov.
[51] Boyd MR, Paull KD. Some practical considerations and applications of thenational cancer institute in vitro anticancer drug discovery screen, Drug Dev.Res. 1995; 34: 91-109.
[52] Monks A, Scudiero D, Skehan P, Shoemaker R, Paull K, Vistica D, Hose C, Langley J, Cronise P, Vaigro-Wolff A, Gray-Goodrich M, Campbell H, Mayo J, Boyd M. Feasibility of a high-flux anticancer drug screen using a diverse panel of cultured human tumor cell lines, J. Nat. Cancer Inst. 1991; 83(11): 757-766.
[53] Shoemaker RH. The NCI60 human tumor cell line anticancer drug screen, Nat. Rev. Cancer. 2006; 6: 813-823.
[54] Boyd MR, Teicher BA. (Ed.), Cancer Drug Discovery and Development, 2, Humana Press, 1997, pp. 23-43.